

# Untargeted Metabolomics and Gut Microbiota Modulation Study of Fermented Brown Rice for Obesity

Kaliyan Barathikannan, Ramachandran Chelliah, Selvakumar Vijayalakshmi, Fred Kwame Ofofu, Su-Jung Yeon, Deuk-Sik Lee, Jong-Soon Park, Nam-Hyeon Kim, and Deog-Hwan Oh\*



Cite This: *ACS Omega* 2024, 9, 37636–37649



Read Online

ACCESS |



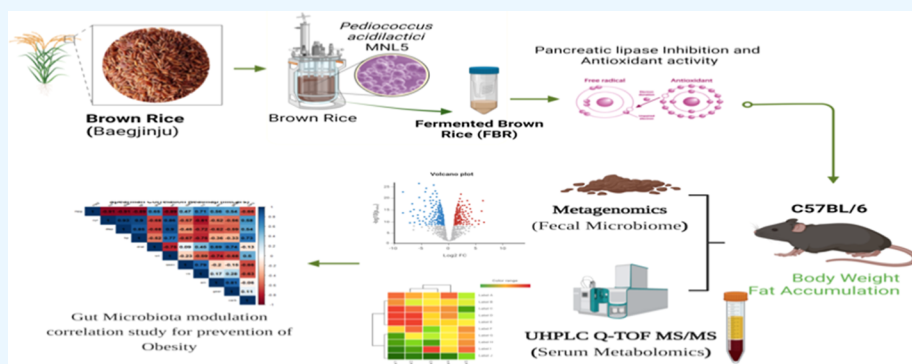
Metrics & More



Article Recommendations



Supporting Information



**ABSTRACT:** Obesity or excess adipose tissue mass increases the risk of heart disease, hypertension, and diabetes. Obesity might be prevented by consuming plant-based probiotic fermented foods. This study aimed to determine whether adding *Pediococcus acidilactici* MNL5 to fermented brown rice (FBR) enhances its metabolites, lipase activity, and antioxidant efficiency. UHPLC–Q–TOF–MS/MS analysis revealed significant changes in untargeted metabolite profiles, while, compared with those of raw brown rice (RBR), FBR contained more antioxidant and lipase inhibitors. We evaluated the FBR in HFD (high-fat-diet)-induced obese mice by employing biochemical, histological, gut microbiome, and serum metabolomics approaches. FBR MD (250 mg/kg) decreased body weight (BW) and fat content compared with RBR. With subsequent FBR MD, mice fed a HFD may have reduced serum lipid levels. A HFD with a mid-dose FBR improved the gut microbiota diversity, composition, and structure; reduced the abundance of obesity-related genera such as *Helicobacter*, *Clostridium*, and *Desulfovibrio*; and promoted the abundance of beneficial genera such as *Bifidobacterium*, *Akkermansia*, and *Lactobacillus*, which are inversely correlated with BW, total cholesterol, TG, LDL-C, and HDL-C. In addition, FBR MD has been associated with increased levels of palmitic acid, EPA, oleic acid,  $\alpha$ -linolenic acid, indole, dodecanoic acid, and amino acids. FBR, in its entirety, has exhibited promise as a functional material for ameliorating obesity.

## 1. INTRODUCTION

Global obesity is a growing health issue, especially in low- and middle-income countries. Obesity has risen in middle- and low-income countries in recent decades, while it has fallen in high-income countries. Overweight and obesity rates in Korea have been steadily increasing, from 19.0% in 2009 to 23.9% in 2019.<sup>2</sup> By the year 2030, one billion individuals will be overweight, with one in seven men and one in five women being overweight, according to the World Obesity Federation.<sup>1</sup> The incidence of metabolic syndrome and its associated consequences, such as cardiovascular disease, cancer, gastrointestinal illness, osteoarthritis, and overall mortality, are both elevated in people who are overweight or obese.<sup>3</sup> Recent research has shown that the high fat content and oxidative stress associated with a Western diet could increase systemic inflammation. The term “western diet” is commonly used to describe a dietary pattern that is high in processed foods, fats,

sugars, and meats, which has been linked to increased oxidative stress. This diet typically leads to an elevated production of free radicals, which are reactive molecules that can damage cells and tissues, contributing to various health issues, including cardiovascular diseases and diabetes.<sup>4</sup> Ancient humans used health-promoting microorganisms to ferment food and beverages. Food-grade healthy microorganisms, nutraceuticals, and bioactive substances are found in fermented foods. These conditions provide a good environment for good bacteria to live in the gut and increase their metabolic activity.

**Received:** February 22, 2024

**Revised:** July 27, 2024

**Accepted:** August 8, 2024

**Published:** August 28, 2024



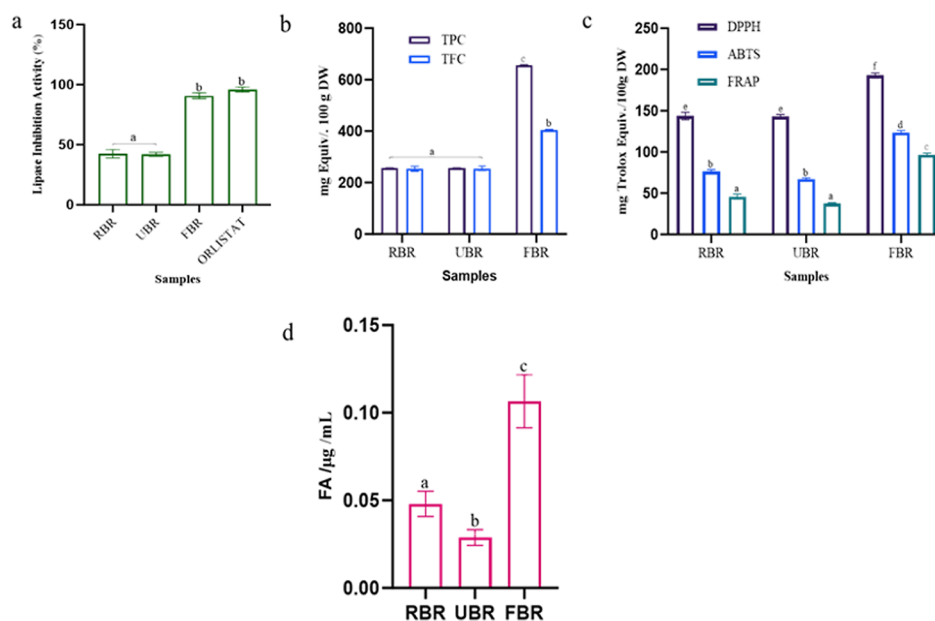


**Figure 1.** Fermentation improves bioactive metabolites and their functional activity compared RBR, UBR, and FBR samples. (a) Lipase inhibition activity, (b) TPC and TFC, (c) antioxidant activity, and (d) FBR 24 h samples were quantification of ferulic acid (indicator compounds) by HPLC method. Different superscripts (a–d) represent significantly different values ( $p < 0.05$ ).

LAB has the most extensive history of usage as probiotics and are a major component of probiotics found in fermented foods. LAB, an abbreviation generally recognized as safe, is the classification given to lactobacilli. The beneficial bacteria *Lactobacillus* and *Pediococcus* can maintain a balanced microbiome in the intestines and control cholesterol functions, specifically cholesterol's involvement in metabolic processes, particularly concerning dietary fat digestion and absorption. Enzymes such as pancreatic lipase and cholesterol esterase are directly involved in breaking down dietary fats, facilitating their absorption in the digestive system.<sup>5</sup> Cereal products are the mainstay of the diets of numerous Asian countries. Prebiotics, which are abundant in cereals, are indigestible dietary components that benefit the host by promoting the expansion and activity of a single or small group of beneficial bacteria in the colon, increasing the overall health of the host. Rice, a member of the grass family (*Oryza sativa* L.), is a staple meal in many countries.<sup>6</sup> Brown rice is rich in antioxidants, nutrients, and other chemical elements that contribute to a nutritious diet. The presence of antioxidants in rice may explain why areas that eat large amounts of brown rice have a lower incidence of chronic diseases, according to epidemiological research.<sup>7</sup>

Solid-state fermentation (SSF) trays are the most common and are inexpensive. To promote the consistent growth of mycelia or other bacteria, these covered metal trays were loosely packed with a solid substrate and inoculum. The production of metabolites requires microbial growth, which is facilitated by SSF.<sup>8</sup> Microbial fermentation is thought to be a more favorable industrial method for producing bioactive compounds than enzymatic fermentation because it is more economical and environmentally friendly.<sup>9</sup> Ultrahigh-performance liquid chromatography tandem mass spectrometry (UHPLC–Q-TOF–MS) is a breakthrough chromatographic technology based on LC–MS that can identify and characterize metabolites with high accuracy. The majority of small-molecular-weight metabolites found in food samples have a

broad dynamic range of concentrations and polarities. Oryzanol, GABA, and ferulic acid, which are found in fermented brown rice (FBR), have several physiological benefits, including a reduction in serum cholesterol.<sup>10,11</sup>

Our previous investigations demonstrated that the release of triglycerides (TGs) into lipid droplets during the accumulation of fat was caused by the inhibition of lipase, which is observed in both humans and *Caenorhabditis elegans*.<sup>12</sup> Probiotic fermentation produced physiologically active compounds derived from brown rice materials may synergistically promote health. Therefore, fermented foods, which add aroma, flavor, and nutrition, are staple components of human diets worldwide. Moreover, bacteria and metabolites from various fermentations can greatly affect human health. A previous study showed that FBR changes the glucose-dependent insulin signaling pathway in *C. elegans*, which controls the metabolism of fats and sugars.<sup>12,13</sup> The fermentation of whole grain cereals into nutritious foods has recently emerged as a fashionable technique. Another exciting development in the health food industry is the use of fermentation biotechnology to make useful products.

The objective of this work was to use *Pediococcus acidilactici* MNLS, a promising probiotic strain, for the development of FBR. The FBR that was developed was evaluated in C57BL/6 mice that were fed a high-fat diet (HFD). This study investigated its impact on maintaining the stability of the gut microbiota and modulating metabolic pathways to prevent obesity.

## 2. RESULTS

**2.1. Fermentation Impact of Raw Brown Rice (RBR) and FBR on Functional Activities.** According to the inhibitory activities of the enzyme and product formation, the percentage of pancreatic lipase activity is shown in Figure 1a. However, the RBR and FBR extracts demonstrated lipase inhibition rates of 42.44 and 90.66%, respectively. The total phenolic content (TPC) and total flavonoid content (TFC) of

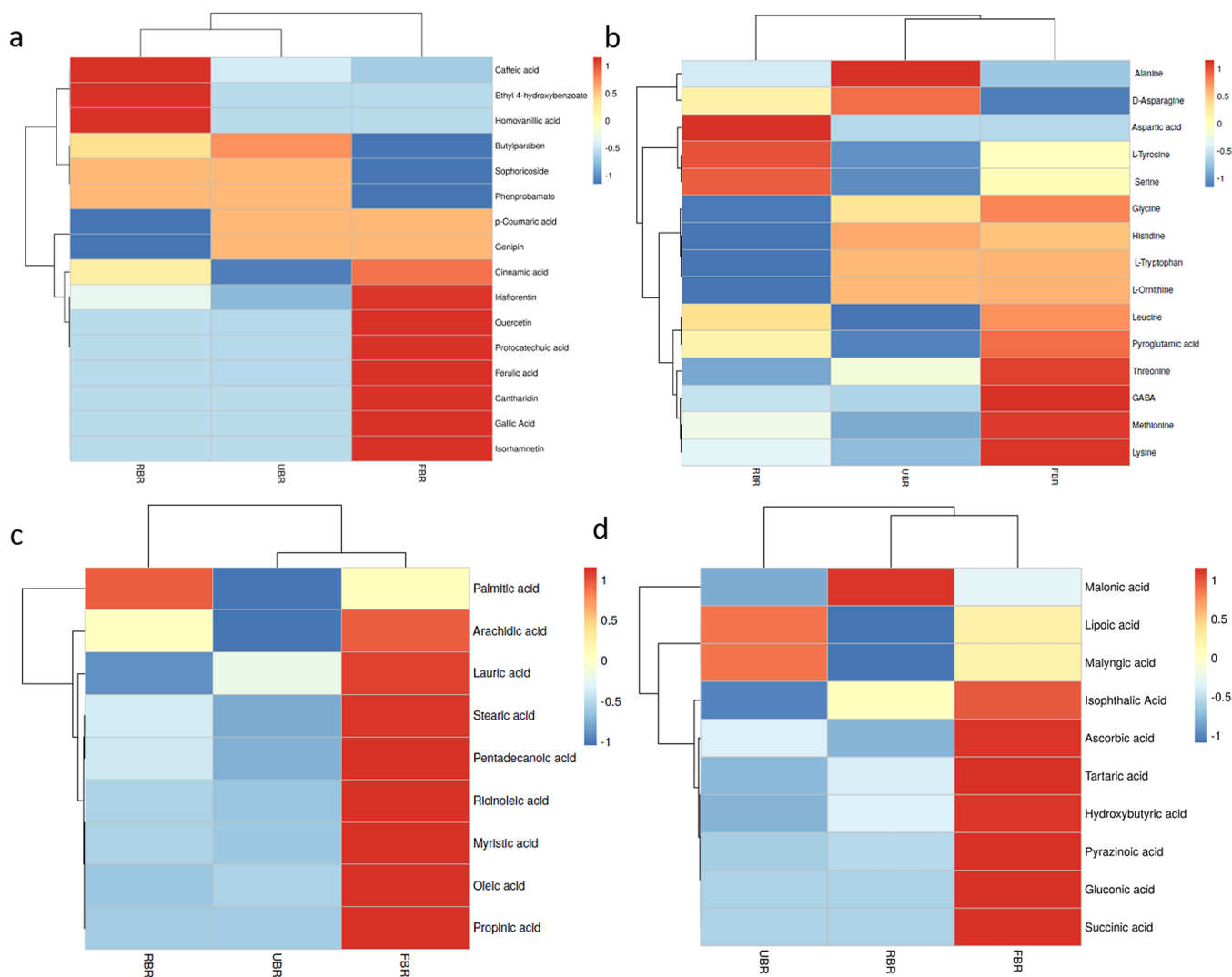


**Figure 2.** Heatmap showing the profiles of the RBR, UBR, and FBR materials. (a) Phenolic compounds, (b) AAs, (c) fatty acids, and (d) organic acids. Heatmap depicts varying levels of metabolites, with blue indicating a lower level and red indicating a higher level.

the raw and FBR products are shown in Figure 1b. The TPC and TFC increased in the FBR products compared to those in the RBR products. After 24 h of fermentation, the highest TPC ( $655.66 \pm 1.81$  mg GA equiv/mg, DW) and TFC ( $402.50 \pm 2.12$  mg CAE equiv/mg, DW) were detected. There was a correlation between the TFC and TPC, which helped determine the antioxidant effect. Our findings indicate that further studies are required to enhance the bioactivity of polyphenols in FBR and improve their antioxidant efficacy. Absorption spectroscopy is among the most widely used methods for assessing the antioxidant activity of natural materials. DPPH activity was greatest in the FBR ( $192.7 \pm 1.8$  mg Trolox equiv/100 g, DW), and the lowest value was detected in the RBR ( $143.6 \pm 1.44$  mg Trolox equiv/100 g, DW). ABTS activity was highest in FBR ( $123.7 \pm 1.99$  mg Trolox equiv/100 g, DW), and RBR had the least activity for ABTS. Similarly, FRAP was greater in the FBR treatment ( $96.5 \pm 1.31$  mg Trolox equiv/100 g, DW) than in the RBR treatment (Figure 1c). FBR has increased levels of bioactive metabolites produced by ferulic acid indicator compounds. Our indicator compound, ferulic acid, was considerably 2-fold more abundant after 24 h of fermentation, according to HPLC quantification than in RBR (Figure 1d). UHPLC–QTOF–

MS/MS analysis of the RBR, UBR, and FBR samples revealed 16 phenolic acids, 15 amino acids (AAs), 9 fatty acids (FAs), and 10 organic acids (Figure 2). Additionally, an untargeted metabolomics study showed that FBR greatly improved the levels of bioactive chemicals such as quercetin, isorhamnetin, cantharidin, irsiflorentin, GABA, stearic acid, and gluconic acid. Based on these results, the difference between the RBR and UBR samples was determined to be negligible. Further analysis was performed with the RBR and FBR groups.

**2.2. FBR Products Reduced Body Weight, Food Intake, Body Fat, and Organ Weight.** Figure 3 shows the changes in the body weight (BW), body mass gain (BMG), food intake, and organ weights. After 11 weeks, the BW of the FBR mid-dose (FBR MD) group was significantly lower than that of the HFD group (Figure 3a,  $p < 0.05$ ). At 11 weeks, the BWs of ND, orlistat, and FBR MD were 30.02, 33.20, and 34.01 g, respectively (HFD group, 43.22 g). As shown in Figure 3b,c, the BMG and food intake of the HFD group were greatest, whereas those of the ND, FBR MD, and orlistat groups were less than those of the HFD group. Figure 3d–f shows that the body fat, liver, and kidney weights were significantly reduced in the FBR MD groups (Figure S1). In particular, the adipose tissue weights of the FBR MD mice

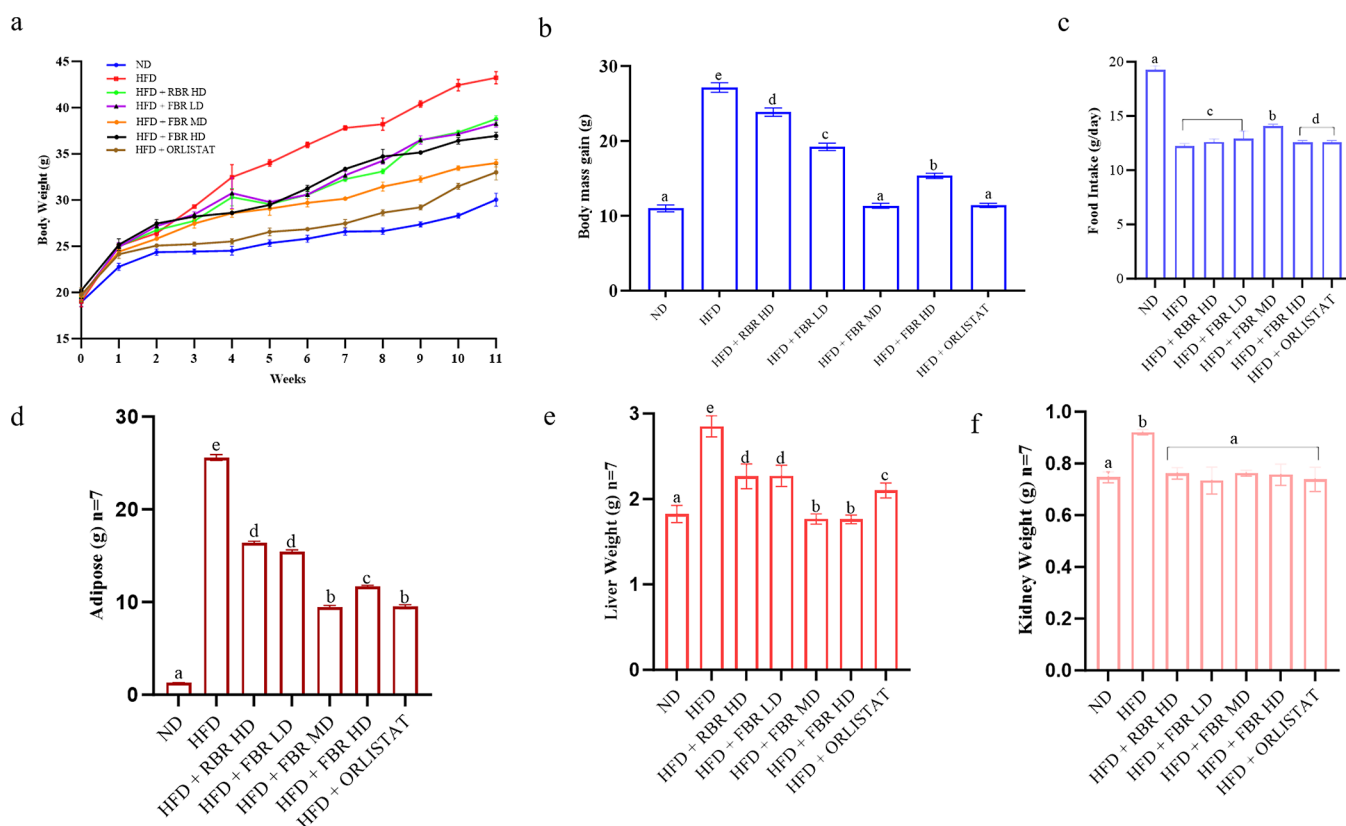


**Figure 3.** FBR improves HFD-induced obesity in mice. Effects of FBR on BW changes: (a) final BW, (b) BMG, (c) food intake, (d) adipose weight ( $n = 7$ ), (e) liver weight ( $n = 7$ ), and (f) kidney weight ( $n = 7$ ). All the data are expressed as the means  $\pm$  SDs ( $n = 7$ ). Different superscripts (a–e) represent significantly different values ( $p < 0.05$ ).

**Table 1.** TG, TC, LDL-C, and HDL-C Levels in Mouse Serum ( $n = 7$ )<sup>a</sup>

treatments	TG (mg/dL)	TC (mg/dL)	LDL-C (mg/dL)	HDL-C (mg/dL)
ND	74.13 $\pm$ 0.35 <sup>b</sup>	172.33 $\pm$ 1.16 <sup>c</sup>	35.00 $\pm$ 0.75 <sup>a</sup>	211.43 $\pm$ 0.35 <sup>d</sup>
HFD	170.70 $\pm$ 0.72 <sup>c</sup>	265.27 $\pm$ 0.80 <sup>d</sup>	52.90 $\pm$ 0.50 <sup>a</sup>	110.40 $\pm$ 0.70 <sup>b</sup>
HFD + RBR HD	124.97 $\pm$ 0.51 <sup>b</sup>	221.20 $\pm$ 1.01 <sup>d</sup>	47.70 $\pm$ 0.60 <sup>a</sup>	187.83 $\pm$ 0.60 <sup>c</sup>
HFD + FBR LD	97.60 $\pm$ 0.82 <sup>b</sup>	201.27 $\pm$ 0.50 <sup>d</sup>	42.73 $\pm$ 0.65 <sup>a</sup>	163.67 $\pm$ 0.55 <sup>c</sup>
HFD + FBR MD	78.50 $\pm$ 0.87 <sup>b</sup>	185.67 $\pm$ 0.74 <sup>d</sup>	37.53 $\pm$ 0.51 <sup>a</sup>	196.77 $\pm$ 0.54 <sup>c</sup>
HFD + FBR HD	87.53 $\pm$ 0.45 <sup>b</sup>	224.70 $\pm$ 0.56 <sup>d</sup>	43.63 $\pm$ 0.71 <sup>a</sup>	174.13 $\pm$ 0.59 <sup>c</sup>
HFD + ORLISTAT	76.03 $\pm$ 0.80 <sup>b</sup>	181.73 $\pm$ 0.70 <sup>c</sup>	37.77 $\pm$ 0.42 <sup>a</sup>	199.63 $\pm$ 0.63 <sup>d</sup>

<sup>a</sup>The values are presented as the means  $\pm$  standard deviations ( $n = 7$ /group). (a–d) Mean values with different letters under the same column are significantly different ( $p < 0.05$ ) according to Duncan's multiple range test.

dramatically decreased. These results suggest that FBR MD decreases BW, body fat, and organ weight and thereby has anti-obesity effects.

**2.3. FBR Products Improve Blood Biochemistry.** In this study, 11 weeks of HFD supplementation caused a statistically significant increase in the levels of serum TG and total cholesterol (TC) compared to those in normal diet-fed mice. The mean changes in TG, TC, high-density lipoprotein cholesterol (HDL-C), and low-density lipoprotein cholesterol (LDL-C) for the different treatment groups are shown in Table 1. The TG, TC, HDL-C, and LDL-C levels in the HFD group (170.70  $\pm$  0.72, 265.27  $\pm$  0.80, 52.90  $\pm$  0.50, and 110.40  $\pm$  0.70 mg/dL, respectively) were significantly different from those in the NC group. After 11 weeks, the FBR MD group showed a significant reduction in plasma TG, TC, HDL-C, and LDL-C (78.50  $\pm$  0.87, 185.67  $\pm$  0.74, 37.53  $\pm$  0.51, and 196.77  $\pm$  0.54 mg/dL, respectively) compared with those of the HFD group. The administration of FBR MD produced a

significant reduction in sugar blood levels compared to those in the HFD group, but an increase in serum TGs was also observed, particularly with RBR intake. The TC concentration tended to decrease in both FBR MD groups compared with that in HFD-fed mice. The HFD group exhibited HDL-C levels higher than those of the other mice groups.

**2.4. Effect of FBR Products on Leptin, Adiponectin, and mRNA Expression of Obesity-Related Genes.** As shown in Figure 4a, the serum leptin level in the HFD group was greater than that in the other groups. The leptin level in the normal group was significantly lower than that in the HFD group. The levels of leptin in the RBR high-dose (HD), FBR low-dose (LD), FBR MD, FBR HD, and FBR ORL groups were significantly lower than those in the HFD group ( $p < 0.05$ ). The levels in the other two groups were also lower than those in the HFD group, indicating that FBR MD had a certain effect on reducing serum leptin levels in obese mice. In addition, the adiponectin levels shown in Figure 4b indicate

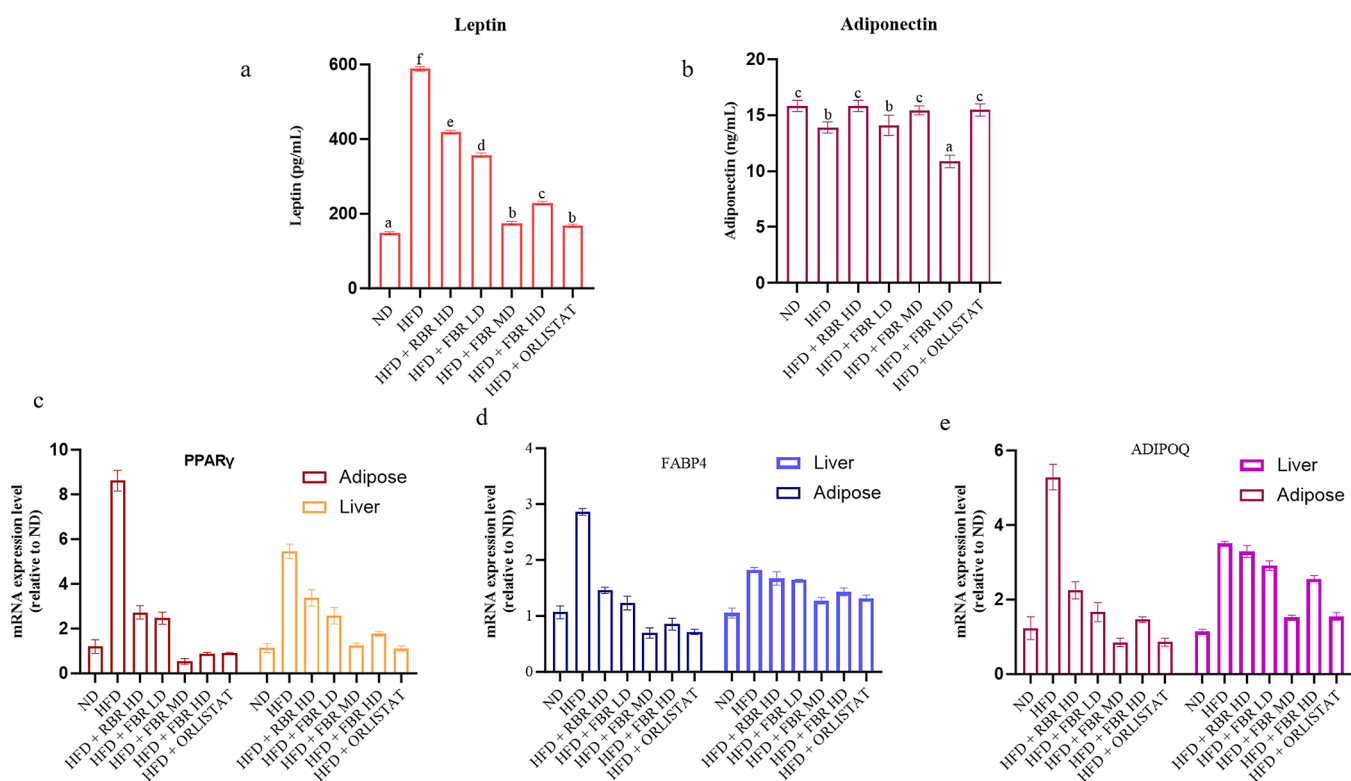


**Figure 4.** FBR improves HFD-induced obesity in mice. (a) Serum leptin, (b) serum adiponectin, (c) mRNA expression of the PPAR $\gamma$  gene in adipose and liver tissue, (d) mRNA expression of the FABP4 gene in adipose and liver tissue, and (e) mRNA expression of the ADIPOQ gene in adipose and liver tissue. All the data are expressed as the means  $\pm$  SDs ( $n = 7$ ). Different superscripts (a–f) represent significantly different values ( $p < 0.05$ ).

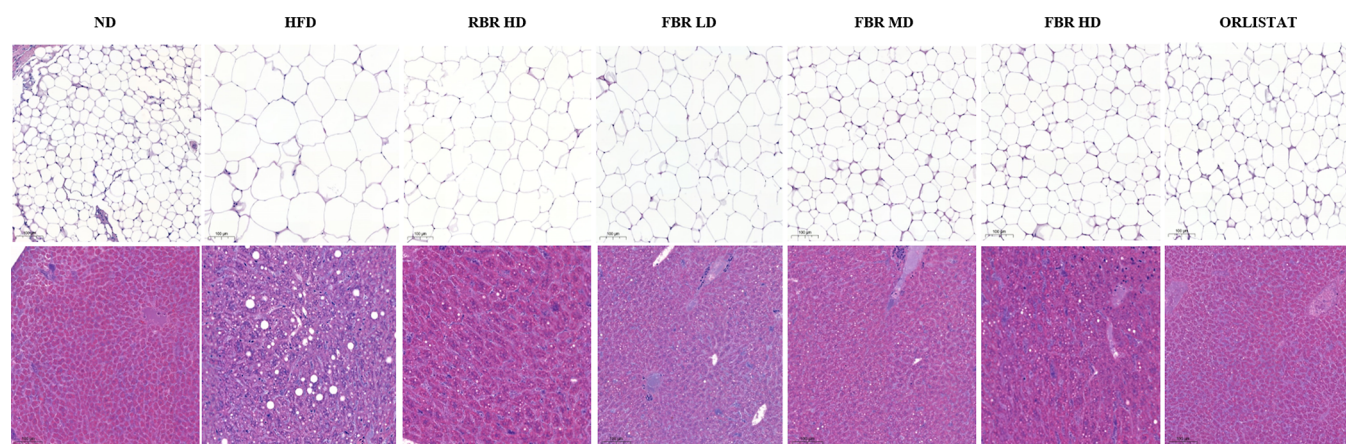


**Figure 5.** Representative hematoxylin and eosin (H&E) staining of liver sections from the ND, HFD, HFD + RBR HD, HFD + FBR LD, HFD + FBR MD, HFD + FBR HD, and HFD + ORLISTAT groups ( $n = 7$ ). (a) H&E staining of adipose tissue at 10 $\times$  magnification; scale bar = 100  $\mu$ m. (b) Liver H&E staining at 10 $\times$  magnification; scale bar = 100  $\mu$ m.

that the levels of ADPN in each of the administration groups and in the normal group were greater than those in the HFD group, and those in the RBR HD, FBR LD, FBR MD, and FBR ORLISTAT groups were significantly greater than those in the HFD group ( $p < 0.05$ ).

We analyzed the expression patterns of obesity-related genes in the liver and adipose tissue to understand the mechanisms by which FBR MD reduces BW gain. In adipose tissue and liver, the mRNA expression of PPAR- $\gamma$  in the FBR MD group was significantly lower than that in the HFD group ( $p < 0.05$ ), whereas the mRNA expression of PPAR- $\gamma$  in the HFD group was considerably greater than that in the ND group (Figure 4c,

$p < 0.01$ ). In addition, the mRNA expression of FABP4 and ADIPOQ in the FBR MD group was approximately 60% lower than that in the HFD group ( $p < 0.01$ , Figure 4d,e), whereas the mRNA expression was lower than that in the RBR group.

**2.5. Effect of FBR Products on Adipose and Liver Histology.** Histological observation of hematoxylin and eosin (H&E)-stained adipose tissue revealed that fat cells in the ND, FBR MD, FBR HD, and orlistat groups were smaller than those in the HFD and RBR HD groups (Figure 5a). Compared with those in the RBR HD group, the size of fat cells in the HFD group increased. This finding indicates that FBR MD treatment effectively reduced fat cell size and reduced

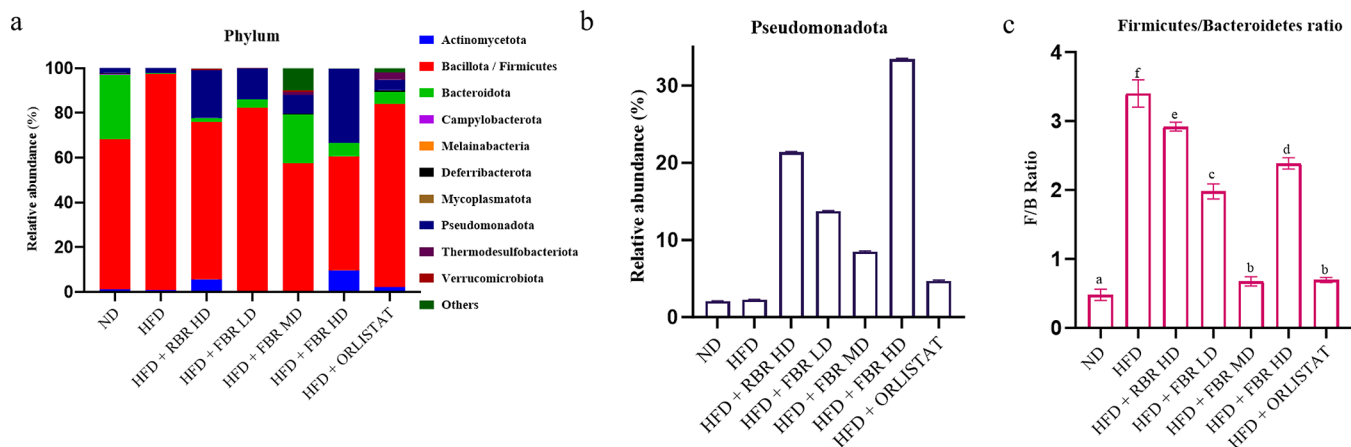


**Figure 6.** FBR improves HFD-induced obesity in the mouse gut microbiota. (a) Phylum-level composition of the gut microbiota in different groups. (b) Order-level composition of the gut microbiota in different groups. (c) Firmicutes/bacteroidetes ratio in different groups [all data are expressed as the mean  $\pm$  SD ( $n = 7$ )]. Different superscripts (a–f) represent significantly different values ( $p < 0.05$ ).

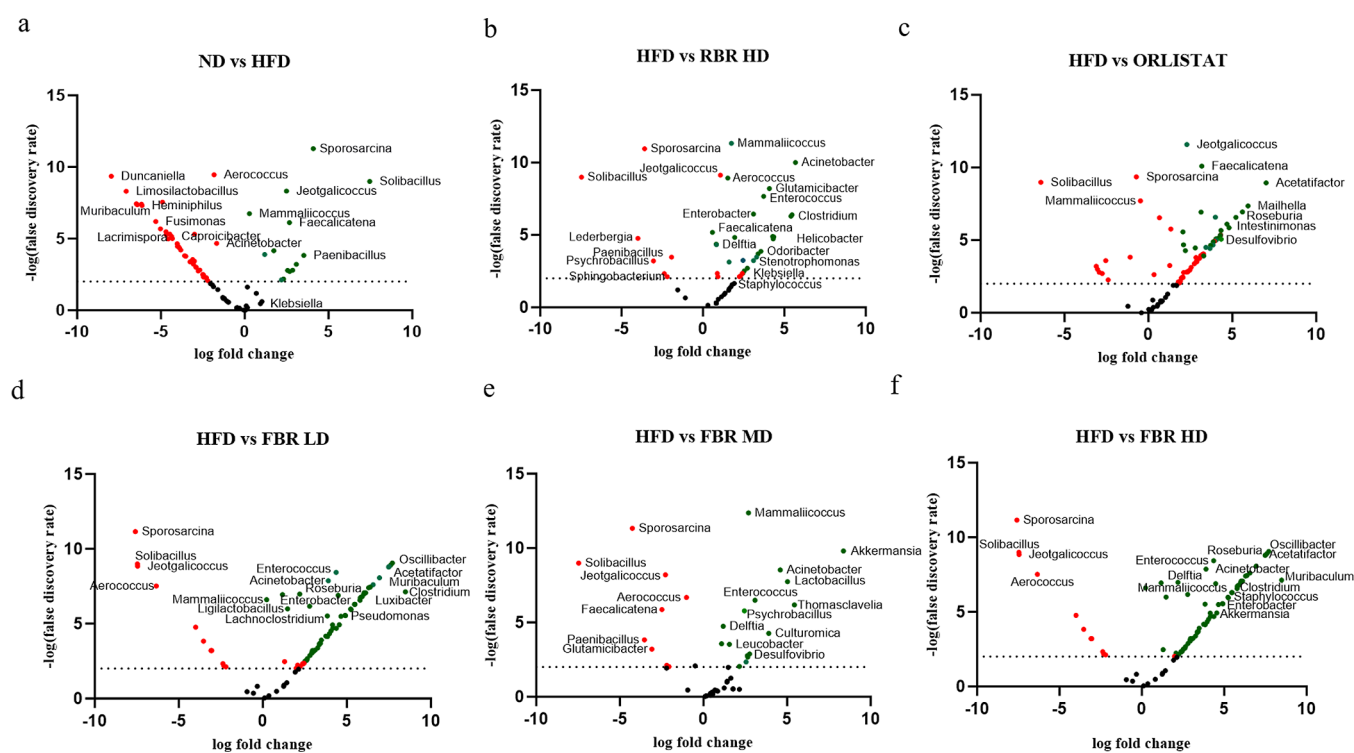


**Figure 7.** FBR improves HFD-induced obesity in the mouse gut microbiota. Volcano plots showing significantly changed microbiome using altered microbiomes according to log fold change and FDR at  $p < 0.01$ . (a) Normal diet group vs HFD-induced mouse group; (b) HFD group vs RBR HD group; (c) HFD group vs ORLISTAT group; (d) HFD group vs FBR LD group; (e) HFD group vs FBR MD group; and (f) HFD group vs FBR HD group. Red dots signify features that are negatively enriched, indicating a downregulation or decrease in the experimental group compared to the control. On the other hand, green dots denote positively enriched features, which suggest an upregulation or increase in the experimental group relative to the control. \*\*\* $p \leq 0.001$ . All the data are expressed as the means  $\pm$  SDs ( $n = 7$ ).

adipocyte size. To confirm whether HFD and FBR MD treatments affect liver fat accumulation, we conducted the histopathological examination of liver tissues stained with H&E, and the results are presented in Figure 5b. The ND group exhibited normal liver architecture and hepatic lobules, whereas the HFD group exhibited hepatocellular steatosis, vacuolization of hepatocytes, and severe accumulation of lipid droplets in hepatocytes, with the nucleus being pushed to the periphery of the hepatocytes. However, FBR MD treatment alleviated the pathological changes in liver tissues; in particular, no obvious lipid droplets were observed in the hepatocytes.

After FBR-induced MD, a significant accumulation of lipid droplets persisted in the hepatocytes, but the fat cell size was significantly reduced compared with that in the HFD group.

**2.6. Impact of FBR on the Gut Microbiota Composition in Obese Individuals.** The gut microbiota composition at week 11 of the intervention was examined using 16S rRNA sequencing. The relative abundance of phylum *Bacillota*/*Firmicutes* significantly increased during the early stages of obesity compared to that in ND-fed (66.83%) and HFD-fed (96.76%) mice. However, the abundance of the phylum *Bacteroidota* was significantly lower in HFD-fed (0.25%) mice

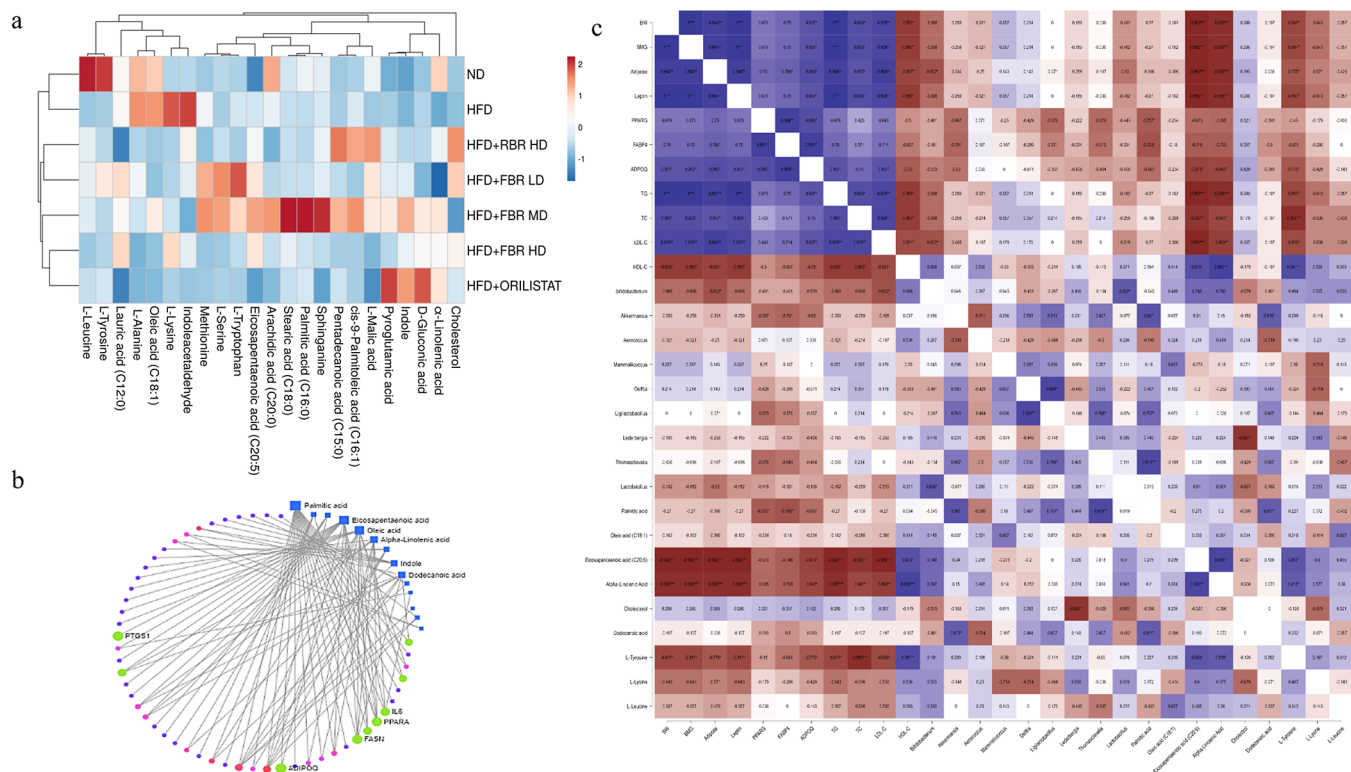


**Figure 8.** FBR improves HFD-induced obesity in a mouse gut microbiota correlation study. (a) Heatmap of the gut microbiota composition in different groups at the genus level. (b) Serum metabolite–gene interaction network [Kyoto encyclopedia of genes and genomes (KEGG) pathway]. (c) Heatmap of the Spearman correlation coefficient between obesity-related physiological traits, genera and significantly changed metabolites.

than in ND-fed (29.09%) mice (Figure 6a). The abundance of the phylum *Pseudomonadota* was significantly lower in HFD-fed mice (2.06%) than in ND-fed mice (2.25%).

Given that mid-dose FBR supplementation (HFD + FBR MD) demonstrated better efficacy than RBR, the other FBR LD and HD groups exhibited better efficacy. At the phylum level, *Bacteroidota*, *Bacillota/Firmicutes*, and *Pseudomonadota* were the most dominant bacteria in the seven groups. The relative abundances of *Bacteroidota*, *Bacillota/Firmicutes*, and *Pseudomonadota* in the NC group were 66.83, 29.09, and 2.06%, respectively. In contrast, HFD feeding increased the relative abundance of *Bacillota* (96.76%) and *Pseudomonadota* (2.25%) but decreased the abundance of *Bacteroidota* (0.25%) at the phylum level. However, compared with those in the HFD group, the abundances of *Bacillota* (57.16%), *Pseudomonadota* (8.39%), *Bacteroidetes* (21.85%), and *Thermodesulfobacteriota* (1.52%) were significantly lower in the HFD + FBR MD group (Figure 5a,b). Orlistat treatment also significantly decreased the relative abundance of *Bacillota* (81.79%) and increased the abundances of *Bacteroidota* (5.49%), *Pseudomonadota* (4.72%), and *Thermodesulfobacteriota* (3.12%).

Moreover, compared with the NC group, the obese group exhibited a markedly increased Firmicutes/Bacteroidetes (F/B) ratio (3.4) (0.48). Nonetheless, the F/B ratio decreased significantly after FBR MD (0.67) and orlistat (0.69) treatment, similar to that in the NC group (Figure 5c). Alpha diversity indices are used to measure the microbial community's richness (Chao1) and diversity (Shannon and Inverse Simpson). Compared with NC, obesity decreased the Chao1 index and increased the inverse Simpson index. However, no significant differences in the Shannon or inverse Simpson indices were observed between the ND and RBR

groups. Compared with the HFD group, the HFD + FBR MD group had decreased Chao1, Shannon, and inverse Simpson indices. In contrast to those in the HFD group, the Chao1 index in the HFD + orlistat group increased, but the Shannon and inverse Simpson indices did not significantly differ (Figure S2).

**2.7. FBR Product-Mediated Modulation of the Gut Microbiota Is Associated with a Reduction in Obesity Risk.** A volcano plot based on the log fold change and false discovery rate (FDR) with a cutoff value of 2 ( $p < 0.01$ ) was used to distinguish the key bacterial groups among the ND-, HFD-, HFD + RBR-, and HFD + FBR-treated groups. The significantly changed genera with respect to obesity were selected based on the FDR ( $p < 0.01$ ). Compared to the diet, HFD consumption significantly affected the composition of the gut bacteria (Figure 7a).

The HFD groups exhibited dysbiosis of the gut microbiota characterized by a noticeable increase in the relative abundance of *Sporosarcina*, *Solibacillus*, *Jeotgaliococcus*, *Mammaliococcus*, *Faecalicatena*, *Delftia*, and *Lederbergia*, in addition to a decrease in the abundance of *Aerococcus*, *Duncaniella*, *Limosilactobacillus*, *Lactobacillus*, *Muribaculum*, *Prevotella*, *Heminiphilus*, *Eubacterium*, *Prevotellamassilia*, and *Paramuribaculum* genera (Figure 7b). RBR HD treatment reversed 10 of the significant changes in genera induced by HFD, including decreased abundances of opportunistic pathogens such as *Sporosarcina*, *Solibacillus*, *Jeotgaliococcus*, *Mammaliococcus*, *Faecalicatena*, *Delftia*, *Lederbergia*, *Helicobacter*, *Roseburia*, and *Psychrobacillus* (Figure 7c). The FBR LD and HD treatments significantly altered the abundance of genera induced by the HFD, including opportunistic pathogens such as *Sporosarcina*, *Solibacillus*, *Jeotgaliococcus*, *Clostridium*, *Helicobacter*, *Aerococcus*, *Roseburia*,

and *Psychrobacillus* (Figure 7d,f). In particular, FBR MD (Figure 7e) significantly increased beneficial genera such as *Bifidobacterium*, *Acinetobacter*, *Akkermansia*, *Thomasclavelia*, *Leucobacter*, and *Streptococcus*. In contrast, there was a decreased abundance of opportunistic pathogens such as *Staphylococcus*, *Sporosarcina*, *Solibacillus*, *Jeotgalicoccus*, *Sphingobacterium*, and the *Helicobacter* genus (Figure S3).

**2.8. Metabolites Associated with Obesity and FBR Supplementation.** Serum metabolomics analysis was performed to explore further the obesity-related signatures mediated by the gut microbiota. Metabolites, including AAs and their derivatives, bile acids, FAs, and vitamins, were identified. The AAs and their derivatives that were more enriched in the HFD group than in the ND group included cholesterol, leucine, tyrosine, alanine, lysine, methionine, L-serine, L-tryptophan, and pyroglutamic acid. In contrast, the concentrations of methionine and lysine were low in the HFD group. In comparison, gluconic acid, lipoic acid, L-malic acid, and sphinganine were enriched in ND. In contrast, linoleic acid,  $\alpha$ -linolenic acid, and eicosapentaenoic acid (EPA) were enriched in ND. In the RBR supplementation groups, lysine, methionine, lipoic acid, L-malic acid, sphingosine, and  $\alpha$ -linolenic acid were enhanced. However, supplementation with FBR decreased the serum levels of leucine, tyrosine, alanine, lysine, methionine, L-serine, L-tryptophan, the microbial metabolite indole acetaldehyde, and indole in HFD-fed obese mice. In particular, FBR MD improved the levels of palmitic acid (C16:0), oleic acid (C18:1), EPA (C20:5), lauric acid (C12:0), arachidic acid (C20:0), pentadecanoic acid (C15:0), and *cis*-9-palmitoleic acid (C16:1) after fermented FBR MD supplementation (Figure 8a).

**2.9. Association of Gut Microbes and Metabolites with Obesity.** Compared with other dietary supplements, brown rice more strongly modulates the gut microbiota, and UHPLC–Q-TOF/MS-based untargeted metabolomics was performed to analyze the regulation of the serum metabolic profile. Importantly, all supplementations altered the serum metabolic profile to a certain degree, especially FBR MD, which was closer to that of the ND group. After comparison with the database, 18 and 24 differentially abundant metabolites in total were identified in the seven groups. There were 23 differentially abundant metabolites shared by the seven comparison groups, including 10 AAs, 9 polyunsaturated acids, 2 lipids, and 2 organic acids. In particular, the metabolites cholesterol, sphingosine, L-lysine, L-alanine, oleic acid, and indole 3-acetaldehyde increased in the HFD-induced obese group. In the RBR groups, the levels of L-malic acid, pentadecanoic acid, and *cis*-9-palmitoleic acid increased. In addition, the number of 8 polyunsaturated FAs (PUFAs) and 6 AAs significantly increased in the FBR MD group. In contrast, palmitic acid, EPA, oleic acid, pentadecanoic acid, and L-tryptophan concentrations were highly increased in the FBR MD groups.

The metabolite gene interaction network (KEGG pathway) revealed that palmitic acid, eicosatetraenoic acid, oleic acid, pentadecanoic acid, L-tryptophan, and L-lysine were strongly correlated with obesity-related genes such as PPAR $\gamma$ , PPAR $\alpha$ , FASN, IL6, PTGS2, and ADIPOQ (Figure 7b). Several studies have shown that gut microbial composition and SCFAs are associated with obesity and related chronic diseases. As shown in Figure 7c, Spearman's correlation analysis was used to determine the relationships between BW, FMG, adipose, leptin, PPAR $\gamma$ , FABP4, ADIPOQ, TG, TC, and LDL-C, which

were positively correlated with the other markers. The genera *Bifidobacterium*, *Akkermansia*, *Ligilactobacillus*, *Thomasclavelia*, *Delfia*, *Mammalicoccus*, and *Lactobacillus* were positively correlated with palmitic acid,  $\alpha$ -linolenic acid, oleic acid (C18:1), and eicosatetraenoic acid (C20:5). In addition, *Lederbergia*, *Thomasclavelia*, and *Lactobacillus* were inversely correlated with cholesterol, dodecanoic acid, L-tyrosine, and L-leucine.

### 3. DISCUSSION

Globally, fermented foods constitute a long-standing and ubiquitous culinary tradition. Fermented foods are widely recognized, prevalent, and diverse.<sup>16</sup> Brown rice that has been fermented tastes better, is better for you, and is easier for your body to absorb beneficial nutrients. According to our prior results, a FBR food supplement or medicine can help people who are overweight [12]. Inhibition of lipase is an efficacious mechanism by which TG absorption can be diminished in patients with hypercholesterolemia.<sup>17</sup> Antioxidants, as previously stated, assist in the prevention of aging, obesity, and diabetes, in addition to the degradation of essential FAs, which have been linked to free radicals.<sup>18</sup> For example, it was found that fermented *L. reuteri* AKT1 brown rice, which is high in antioxidant phytonutrients and functional foods that can help with stress alleviation and antioxidants, could improve health.<sup>7</sup> FA enhances antioxidant capacity<sup>19</sup> by exerting a substantial impact on lipid levels in the blood, liver, and skeletal muscle. The potential intracellular mechanisms by which FA prevents metabolic syndrome and influences metabolic diseases through lipid and glucose pathways are revealed. According to Al-Okbi et al.,<sup>20,21</sup> FA enhances glucose and lipid balance in HFD-induced obese mice by regulating hepatic lipid metabolism and gluconeogenic genes. Increasing FA levels increase antioxidant activity, which in turn decreases fat storage, body mass, and hyperlipidemia in overweight mice.<sup>22</sup> In most cases, lipid accumulation is caused by reactive oxygen species, which are detrimental to human health.<sup>23</sup> Previous studies have demonstrated that lipid metabolism genes, including MNLS FBR, can inhibit lipid accumulation in *C. elegans* and extend their life span. Furthermore, our study showed that FA may be successfully detected by the analysis of FBR metabolites that display advantageous characteristics.

Our prior research comparing the HFD group to the ND and FBR groups after 11 weeks revealed that the HFD group experienced a substantial increase in BW gain, which caused obesity. An HFD additionally led to hyperlipidemia in mice, resulting in significant increases in blood TC, TG, and LDL-C. HFDs are known to contribute to lower HDL-C levels, which are crucial for removing cholesterol from the bloodstream and transporting it to the liver for excretion. The decrease in HDL-C associated with HFD intake is a significant factor in the increased risk of cardiovascular diseases. HDL-C, often referred to as “good” cholesterol, plays a crucial role in reversing cholesterol transport, carrying cholesterol away from arteries and back to the liver, where it is processed and excreted. The upregulation of HDL-C in the MD group can be attributed to the dietary composition of this group, which was designed to be lower in fats and higher in fibers and other nutrients known to promote higher HDL-C levels.<sup>24</sup> Administering FBR greatly decreased the weight gain and serum fat levels. An improved effect of FBR MD was observed, leading to a reduction in weight gain and a decrease in serum TG and TC levels to normal levels. Additionally, the



epididymal adipose tissue and liver coefficients may be enhanced by FBR supplementation. Abnormal serum lipid levels are widely recognized as a significant risk factor for the development of CVD. Following the induction of hyperlipidemia by HFD feeding, the risk of cardiovascular disease increases in mice.<sup>24</sup> An abnormal blood lipid level could be corrected by supplementation with FBR MD, which would lower the risk of cardiovascular disease. According to the results of H&E staining, FBR MD demonstrated that HFD feeding resulted in lipid deposition in the liver and adipocyte expansion in subcutaneous fat tissue. Cao et al.<sup>25</sup> reported that Peanut-natto (peanut with *Bacillus subtilis*) fermented material diets can alleviate obesity-induced fat cell accumulation. Our findings demonstrated that FBR MD might significantly downregulate ADI-POQ, FABP4, and PPAR- $\gamma$  mRNA levels in both adipose and liver tissue. By controlling lipolysis and lipogenesis signaling at the transcriptional level, FBR is likely able to alleviate lipid disorders in the liver and adipose tissue of HFD-fed mice, given the above-mentioned important mRNA expression in lipid metabolism. The present study observed a reduction in adiponectin mRNA expression in adipose tissue; the serum levels of adiponectin were found to be significantly higher in the MD group compared to those in the HFD group. This apparent contradiction can be attributed to post-transcriptional modifications and the stability of the adiponectin protein in the bloodstream. Adiponectin has a relatively long half-life in circulation, and its levels can be influenced by factors such as its rate of clearance from the blood, which might be altered in different dietary conditions.<sup>26</sup>

Moreover, the interaction among flavonoids, phenolic compounds, and gut microbiota is believed to influence the overall microbial balance in the gut, potentially reducing the abundance of pathogenic bacteria and enhancing gut health. By altering the microbial landscape in such a manner, flavonoids and phenolics could contribute to better metabolic profiles and reduced inflammation.<sup>27</sup> A gut microbiome dysbiosis signature of obesity is a smaller abundance of Bacteroidetes and an increase in Proteobacteria and Firmicutes at the phylum level.<sup>28</sup> Firmicutes and Proteobacteria were found in greater numbers in our study, along with a higher F/B ratio, which was also observed in studies of obese people than in those of healthy people.<sup>29–33</sup> Adding FBR, on the other hand, greatly reduced the number of these groups of obese people. According to reports, the proinflammatory action of the pathogenic *Helicobacter* genus *Clostridium*, which is a member of the *Pseudomonadota* phylum, has a role in the development of obesity. The fermentation process can modify the gut environment by altering the pH and producing various bioactive compounds, which may favor the growth of certain bacterial taxa, such as *Pseudomonadota*. These bacteria are known for their adaptability to different environments and their ability to metabolize a wide range of organic compounds, which might be more prevalent in the FBR MD diet due to the fermentation of brown rice. FBR MD, which includes higher fiber content and a variety of phytochemicals from both brown rice and its fermentation products, likely supports the growth of diverse microbial communities. Specific bioactive compounds, such as phenols and organic acids, resulting from fermentation may enhance the proliferation of *Pseudomonadota*. These compounds can serve as energy sources for *Pseudomonadota*, enabling them to thrive in the gut ecosystem enriched by a moderate, diverse diet.<sup>34</sup> The microbiome profiles associated with metabolic diseases include, at the genus

level, decreased levels of butyrate-producing bacteria and increased abundances of opportunistic pathogens such as *Jeotgalicoccus*, *Mammaliococcus*, *Aerococcus*, and *Enterococcus*.<sup>35</sup> Some opportunistic pathogens, such as *Jeotgalicoccus*, *Mammaliococcus*, *Aerococcus*, *Enterococcus*, *Clostridium*, and *Helicobacter*, became much less common when people ate FBR. On the other hand, *Lactobacillus*, *Bifidobacterium*, *Akkermansia*, *Ligilactobacillus*, and *Parabacteroides* grew and became more common at the genus level.

Our results showed that following FBR treatment in obese individuals, the levels of circulating indole, *cis*-9-palmitoleic acid, pentadecanoic acid, eicosatetraenoic acid, palmitic acid, arachidic acid, L-tryptophan, L-serine, and methionine increased. Integrating transcriptome and metabolome data at the pathway level revealed the relationships between DEGs and differentially abundant metabolites. According to the KEGG gene–metabolite interaction analysis, five DEGs (FASN, PPAR $\gamma$ , IL6, PTGS1, and ADIPOQ) and six different metabolites (palmitic acid, eicosatetraenoic acid, oleic acid,  $\alpha$ -linolenic acid, indole, and dodecanoic acid) were prevalent in important pathways correlated with obesity. KEGG analysis of the gut microbiota revealed that after different treatments, metabolic pathways for AAs, PUFAs, and lipids were mostly improved. Administration of FBR MD partially reversed the long-term HFD-induced suppression of gluconeogenesis and the promotion of glycolysis, thereby affecting carbohydrate metabolism. HFD-induced imbalances in AA metabolism can lead to a variety of health concerns. In the presence of HFD, the immunological compartment experiences an increase in both its number and its potential for inflammation factors in individuals with obesity.<sup>36–38</sup> An additional finding shows that fat can lead to problems with lipid metabolism, a very important and complicated biochemical process. Thus, by altering the gut microbe balance, FBR MD treatment might help alleviate metabolic problems resulting from a HFD. The physiological roles of a growing number of functional components (such as organic acids, phenolic compounds, polysaccharides, and proteases) of fermented foods are being investigated; of particular relevance are the antiobesity effects and related consequences.<sup>39–41</sup>

The findings show a significant association between almost all differentially abundant metabolites and differential microbiota, as assessed by linking the latter to gut bacteria at the genus level. In particular, *Akkermansia*, *Bifidobacterium*, *Ligilactobacillus*, and *Thomasclavelia* were strongly linked to the main-stream molecules cholesterol and L-lysine, which were downregulated by FBR MD. This leads us to believe that the ability of FBR MD to protect against obesity is due to their ability to ameliorate gut microbial diseases and the changes they cause in metabolic pathways and different metabolites. Significantly, we discovered that the FBR treatment markedly elevated several of the differentially abundant metabolites, such as palmitic acid, oleic acid, eicosatetraenoic acid, and  $\alpha$ -linolenic acid. The outcomes suggested the potential advantages of the optimized FBR dosage for maintaining gut microbiota stability and modifying the metabolic pathways that prevent obesity.

#### 4. CONCLUSIONS

In summary, our findings indicate that FBR treatment reduced the BW produced by HFD consumption and biomarkers associated with obesity. FBR MD reduced the F/B ratio, enhanced the diversity of the gut microbiota, and improved the

structure of the gut microbiota in HFD-fed mice, all of which play roles in the prevention of obesity. The relative abundances of beneficial bacteria such as *Lactobacillus*, *Bifidobacterium*, and *Akkermansia* were greater than those of pathogenic bacteria such as *Clostridium* and *Helicobacter*. According to Spearman's correlation analysis, metabolic profiles are linked to the gut microbiota. A reduction in fat accumulation, hepatic steatosis, and chronic inflammation resulting from feeding mice a HFD was positively correlated with the antiobesity effects of FBR. The gut microbiota modestly controlled the antiobesity efficacy of FBR MD through its inhibition of lipid metabolism. In addition, clinical research is necessary to confirm and investigate the underlying molecular mechanism and regulate metabolic interactions between gut microbes and host physiology in association with the administration of fermented functional brown rice products for the treatment of obesity.

## 5. METHODS

**5.1. Chemicals and Cultures.** Daejung Chemicals and Metals Co., Ltd., Siheung-si, Gyeonggi-do, South Korea, provided MRS broth, Tryptic Soy Broth, peptone and agar, ethanol, methanol, 2-propanol, DMSO, acetonitrile, and nutritional media. NaCl, monopotassium phosphate, dipotassium phosphate, sodium chloride, sodium dihydrogen phosphate, sodium carbonate, potassium persulfate, sodium citrate, 2,2-diphenyl-1-picrylhydrazyl (DPPH), 2,2'-azinobis(3-ethylbenzothiazoline-6-sulfonic acid (ABTS)), methyl cellosolve, Folin–Ciocalteu reagent, triton-X100, ferulic acid, gallic acid, catechin, lipase from porcine pancreas, PicoSens TG, TC, HDL, and LDL/VLDL assay kits were purchased from BIOMAX, Korea. All reagents were of analytical grade. Mouse leptin (ab100718) and mouse adiponectin (ab226900) ELISA kits were obtained from Abcam, Cambridge, UK. All of the analytical reagents were obtained from South Korea.

**5.2. Preparation of FBR.** A brown rice sample (Variety-Baegjinju; *O. sativa* L.) was purchased from a local market in Chuncheon, Republic of Korea. Brown rice (10 kg) was soaked in water at  $20\text{--}25 \pm 2$  °C for 6 h at a 1:1 ratio. After washing, the samples were autoclaved at 121 °C for 15 min and cooled to 40–42 °C. *P. acidilactici* MNLS ( $1.0 \times 10^7$  cfu/g lyophilized powder) and 1% dry brown rice preparation were used to inoculate brown rice samples before steaming. Twenty-four hour tray fermentation was conducted at 37 °C. The FBR was dried in a JSON-050 drying oven at 60 °C for 6 h after 24 h of fermentation. FBR samples were dried and processed into a fine powder using an electric crusher and separated by 20–30  $\mu\text{m}$ . Following drying, the FBR was stored at  $-20$  °C until use.

**5.3. Validation of FBR Materials.** The raw and FBR materials were investigated with an in vitro product validation study using 70% ethanol extraction at a concentration of 1 mg/mL.

**5.3.1. Total Phenolic Content and Total Flavonoid Content.** The TPC and TFC of the FBR samples were assessed using a 36-well plate, following the approach outlined by Barathikannan et al.<sup>12</sup> For the TPC analysis, 200  $\mu\text{L}$  of Folin–Ciocalteu reagent was applied to 100  $\mu\text{L}$  of sample extract, standard, or 95% (v/v) methanol as a blank. After vortexing, the mixture was incubated at ambient temperature for 2 h. Following the addition of 800  $\mu\text{L}$  of 700 mM sodium carbonate to each mixture, the absorbance was measured at 765 nm.

The TFC was prepared by pipetting 250  $\mu\text{L}$  of sample extracts into microplate wells, followed by 75  $\mu\text{L}$  of  $\text{NaNO}_2$  ( $50 \text{ g L}^{-1}$ ) and 1 mL of distilled water. After settling for 5 min, 75  $\mu\text{L}$  of  $\text{AlCl}_3$  (100 g/L) was added. The reaction mixture was allowed to settle before adding 500  $\mu\text{L}$  of 1 M NaOH and 600  $\mu\text{L}$  of distilled water, and the mixture was then incubated for 6 min. After 30 s of shaking, the absorbance at 510 nm was measured by a SpectraMax i3 plate reader (Molecular Devices Korea, LLC, Seoul, Korea). The TPC and TFC values were presented as gallic acid and catechin equivalents per 100 g ( $\text{mg}/100 \text{ g, DW}$ ).

**5.3.2. DPPH, ABTS, and FRAP Radical Scavenging Effects.** For the antioxidant capacity evaluation, DPPH, ABTS, and FRAP assays were conducted. A 500  $\mu\text{M}$  DPPH solution was added to 100  $\mu\text{L}$  of sample in a 24-well plate and incubated for 30 min at room temperature, and the absorbance was read at 515 nm. ABTS solution was prepared by mixing 2.45 mmol/L potassium persulfate with 7 mmol/L ABTS and left in the dark for 12–16 h. This was then diluted to an absorbance of  $0.700 \pm 0.020$  at 734 nm and mixed with sample extracts, and the absorbance was measured. For the FRAP assay, samples were mixed with acetate buffer, TPTZ solution, and  $\text{FeCl}_3 \cdot 6\text{H}_2\text{O}$ , incubated at 37 °C for 10 min, and the absorbance was read at 593 nm. All absorbance measurements were performed using the SpectraMax i3 plate reader, and results were expressed in milligrams of Trolox equivalents per 100 g of dry weight.

**5.3.3. UHPLC-Q-TOF-MS<sup>2</sup> Phenolic Compound Identification.** A combination of UHPLC–Q-TOF–MS<sup>2</sup> was used for the LC–MS<sup>2</sup> analyses. The UHPLC was manufactured by SCIEX and was equipped with the following components: an AD pump, a degasser, an AD autosampler, an AD column oven, and a photodiode array (PDA) detector (ExionLC). An autosampler was used to inject the sample (10  $\mu\text{L}$ ), which was eluted through a binary mobile phase column that contained solution A (water containing 0.1% formic acid) and solution B (methanol). The use of a linear gradient with a flow rate of 0.4 mL/min was programmed for 25 min as follows: 0–3.81 min, 9 to 14% B; 3.81–4.85 min, 14 to 15% B; 4.85–5.89 min, 15% B; 5.89–8.32 min, 15 to 17% B; 8.32–9.71 min, 17 to 19% B; 9.71–10.40 min, 19% B; 10.40–12.48 min, 19 to 26% B; 12.48–13.17 min, 26 to 28% B; 13.17–14.21 min, 28 to 35% B; 14.21–15.95 min, 35 to 40% B; 15.95–16.64 min, 40 to 48% B; 16.64–18.37 min, 48 to 53% B; 18.37–22.53 min, 53 to 70% B; 22.53–22.88 min, 70 to 9% B; and 22.88–25.00 min, 9% B. For the positive ion mode, the capillary temperature and voltage of the sheath gas flow were set at 40 arb. units, and an aux gas flow of 8 arb. units were used. The spray voltage was set at 3.6 kV, and the tube lens voltage was set at 120 V. In negative ion mode, the capillary temperature and voltage were set at 320 °C and  $-40$  V, respectively. The sheath gas flow was set at 40 arb. units, and the gas flow was set at 8 arb. units. The spray voltage reached 2.7 kV, and the tube lens voltage reached  $-120$  V. Fourier transform mass spectrometry in full-scan ion mode was employed to investigate both the positive and the negative ion modes. The spectra were acquired in centroid mode, and the mass scan range was 115–1000  $m/z$  with a resolution of 30,000 full width at half-maximum (fwhm's). The scanning time was approximately 1 s under these conditions. To identify phenolic compounds, spectral evidence from the literature and spectral libraries, such as XCMS Online (Metlin) (<https://metlin.scripps.edu>) and Metabolomics Workbench (<https://www>

metabolo-micsworkbench.org), were compared with retention time and UHPLC–Q–TOF–MS<sup>2</sup> data.

**5.4. Animals and Experimental Design.** This study followed all protocols established by the UK/EU/US Animal Research Reporting In Vivo Experiment and used a four-week-old male C57BL/6J mice. The mice were procured from Nara-Biotechnology Inc. in Seoul, Korea, and were authorized by the Institutional Animal Care and Use Committee of Kangwon National University in South Korea (Approval no. KW-230629-1). In a temperature- and humidity-controlled room with distilled water and food available at all times, the mice were kept in polysulfone boxes with vents. The 49 mice were randomly divided into two groups: the ND group, which consisted of 7 mice, and the HFD group, which included 42 mice, after an acclimation period of 1 week. During the trial, the mice in one group were fed a regular chow diet with 10% fat calories, while those in the other group were fed a HFD with 60% fat calories (D12492).

There were 7 HFD groups, including an obesity control group (HFD group) and a group of HFD-fed mice that were given 500 mg/kg/bw RBR (RBR HD). Four groups of HFD-fed mice were studied: those given 100 mg/kg/bw FBR (LD), 250 mg/kg/bw FBR (MD), 500 mg/kg/bw FBR (HD), or 100 mg/kg/bw orlistat (ORLISTAT). At the same feeding frequency as the other treatment groups, mice in the ND and HFD groups were given 5 mL/kg/bw of normal saline (PBS) via oral gavage once a day for 8 weeks. Every week after the fifth week, BW, food intake, and TC were checked. For microbiota research, fecal samples were frozen at –80 °C and frozen at the beginning and end of the experiment. After the intervention, the mice were fasted for 6 h. Blood samples were collected and centrifuged for 10 min at 3000 rpm. The adipose, serum, and liver tissues were collected and stored at –80 °C until further analysis.

**5.5. Biochemical Analyses.** In summary, blood samples were collected from the tail after the fifth week, and the BeneCheck Supreme Multimonitoring System was utilized to determine the TC level. Serum was extracted from blood collected from the left ventricle at the final stage of the investigation using centrifugation at 1300g at 4 °C for 15 min. The concentrations of HDL, LDL, TG, and TC in the serum were determined in accordance with the manufacturer's instructions using a BIOMAX (Seoul, Korea).

**5.6. Serum Hormones.** The adiponectin (ab108785) and leptin (ab199082) concentrations were determined by using ELISA kits from Abcam (Cambridge, UK).

**5.7. Real-Time Polymerase Chain Reaction (RT-PCR) Analysis.** For RNA extraction, 50 to 100 mg of fat and liver tissue was mixed with 1 mL of TRIzol reagent (TRIzol Thermo Fisher Scientific, Inc., Middletown, VA), and 2 mL of Lysing Matrix S metal beads (MP Biomedicals, Irvine, CA, USA) was added. The mixture was vortexed for 5 min. The fat tissues that had been homogenized were allowed to cool to ambient temperature for 5 min before being centrifuged at 12,000g and 4 °C for 5 min. This high-capacity cDNA synthesis was carried out using the Super Script III First-Strand Synthesis System (Thermo Fisher Scientific, Inc., Middletown, VA) according to the manufacturer's instructions. We measured gene expression using the GoTaq qPCR Master Mix Kit from Promega and the Step One Real-Time PCR Kit from Applied Biosystems in Foster City, CA. For each reaction, 10  $\mu$ L of the GoTaq qPCR Master Mix Kit (A600A), 1  $\mu$ L of cDNA (10 ng  $\mu$ L<sup>-1</sup>), 1  $\mu$ L of each primer (10 pg  $\mu$ L<sup>-1</sup>), and 7

$\mu$ L of nuclease-free water were used. Gene expression levels were normalized to those of the GAPDH primer using the 2<sup>- $\Delta\Delta$ CT</sup> method.<sup>12</sup>

**5.8. Histopathological Observation of Adipose and Liver Tissues.** The adipose tissues and liver tissue were fixed with 10% neutral buffered formalin and subjected to histochemistry as previously described.<sup>14</sup> The tissues were subjected to examination using an optical microscope at 20 $\times$  magnification (Olympus, Japan) and stained with H&E.

**5.9. Sample Preparation and Metabolomics Analysis.** Two hundred microliters of serum were added to 200  $\mu$ L of 70% methanol and vortexed for 2 h at room temperature. The supernatant was filtered through a 0.45  $\mu$ m membrane filter prior to metabolomics analysis via UHPLC–Q–TOF–MS/MS (AB SCIEX XS00R QTOF). The mixture was subsequently centrifuged at 10,000 rpm for 10 min at 4 °C. With a range of 100 to 1000 masses, the negative mode of the Q–TOF–MS<sup>2</sup> instrument was calibrated with a precision of 5000. Following our previous procedure, the samples were placed in an autosampler and subjected to an Accucore C18 analytical column with a binary mobile phase [water containing 0.1% formic acid (A) and methanol (B)]. The identification of metabolites was achieved through the comparison of UHPLC–Q–TOF–MS<sup>2</sup> data with the HMDB and METLIN online spectral databases.<sup>15</sup> Metabolomic KEGG network analysis of functional obesity genes was performed with MetaboAnalyst 6.0 (<https://www.metaboanalyst.ca/MetaboAnalyst/>).

**5.10. Gut Microbiota Analysis.** As detailed in our earlier paper,<sup>15</sup> 16S metagenomic sequencing was carried out at MacroGen, Inc. (Seoul, South Korea) using the Hercules II Fusion DNA Polymerase Nextera XT Index Kit V2 in accordance with the manufacturer's instructions (Illumina). Briefly, for the construction of the sequence library, fecal genomic DNA was isolated, quality controlled, and arbitrarily fragmented, after which 5' and 3' adapter ligation was performed. PCR was used to amplify adapter-ligated fragments, which were then gel purified. After fragments are inserted into a flow cell, bridge amplification is used to generate the clonal clusters. For exact base-by-base sequencing, the library that had been prepared was sequenced on the Illumina MiSeq platform, and the raw data were turned into FASTQ.

**5.11. Statistical Analysis.** The analysis of the data was conducted using GraphPad Prism 10.1.2 (GraphPad Software, San Diego, USA). The outcomes are shown as the average plus or minus the SD from at least three separate analyses, which were determined using one-way analysis of variance and Tukey's test at a significance level of  $p < 0.05$ . For volcano plots, a FDR of  $p < 0.01$  was considered to indicate statistical significance. Parameters were compared using Spearman's correlation analysis at three levels of significance: \* $p < 0.05$ , \*\* $p \leq 0.01$ , and \*\*\* $p \leq 0.001$ .

## ■ ASSOCIATED CONTENT

### SI Supporting Information

The Supporting Information is available free of charge at <https://pubs.acs.org/doi/10.1021/acsomega.4c01203>.

Dissection procedure on 11th week FBR treatments; FBR improves HFD-induced obesity in mice gut microbiota - Cho, Shannon, Inverse Simpson Index, and Alpha rarefaction plots of identified species/OTU; and FBR improves HFD-induced obesity in mice gut

microbiota - Weighted Unifrac PCoA Plot, Phylogenetic tree, Heatmap of gut microbiota composition in different groups a genus level (PDF)

KEGG network analysis (XLSX)

## AUTHOR INFORMATION

### Corresponding Author

**Deog-Hwan Oh** – Department of Food Science and Biotechnology, College of Agriculture and Life Sciences, Kangwon National University, Chuncheon 24341, Republic of Korea; Future F Biotech Co., Ltd., Chuncheon 24341, South Korea; Kangwon Institute of Inclusive Technology KIIT, Kangwon National University, Chuncheon 24341, Republic of Korea; [orcid.org/0000-0002-7472-0436](https://orcid.org/0000-0002-7472-0436); Phone: +82 33 250 6457; Email: [deoghwa@kangwon.ac.kr](mailto:deoghwa@kangwon.ac.kr); Fax: +82 33 259 5565

### Authors

**Kaliyan Barathikannan** – Department of Food Science and Biotechnology, College of Agriculture and Life Sciences, Kangwon National University, Chuncheon 24341, Republic of Korea; Saveetha School of Engineering, Saveetha University, Chennai 600077 Tamil Nadu, India

**Ramachandran Chelliah** – Department of Food Science and Biotechnology, College of Agriculture and Life Sciences, Kangwon National University, Chuncheon 24341, Republic of Korea; Future F Biotech Co., Ltd., Chuncheon 24341, South Korea

**Selvakumar Vijayalakshmi** – Department of Food Science and Biotechnology, College of Agriculture and Life Sciences, Kangwon National University, Chuncheon 24341, Republic of Korea

**Fred Kwame Ofori** – Department of Food Science and Biotechnology, College of Agriculture and Life Sciences, Kangwon National University, Chuncheon 24341, Republic of Korea

**Su-Jung Yeon** – Department of Food Science and Biotechnology, College of Agriculture and Life Sciences, Kangwon National University, Chuncheon 24341, Republic of Korea; Life Science Institute, Well-being LS Co., Ltd., Gangneung 25451, Republic of Korea

**Deuk-Sik Lee** – Life Science Institute, Well-being LS Co., Ltd., Gangneung 25451, Republic of Korea

**Jong-Soon Park** – Life Science Institute, Well-being LS Co., Ltd., Gangneung 25451, Republic of Korea; [orcid.org/0000-0002-0313-2717](https://orcid.org/0000-0002-0313-2717)

**Nam-Hyeon Kim** – Department of Food Science and Biotechnology, College of Agriculture and Life Sciences, Kangwon National University, Chuncheon 24341, Republic of Korea

Complete contact information is available at: <https://pubs.acs.org/10.1021/acsomega.4c01203>

### Author Contributions

Conception and design of the study were carried out by K.B., R.C., and S.V. Acquisition of data was done by K.B. and R.C. Analysis and interpretation of data were done by K.B., R.C., S.V., and F.K.O. Drafting the article was done by K.B. and R.C. D.H.O. revised the content. K.B., S.J.Y., D.S.L., J.S.P., N.H.K., and H.H.O. approved the final version of the manuscript. D.H.O. and D.S.L. performed the funding acquisition.

### Funding

This research was financially supported by the Ministry of SMEs and Startups (MSS), Korea, under the “Regional Specialized Industry Development Program (R&D, Grant no. S3272987)” supervised by the Korea Technology and Information Promotion Agency for SMEs (TIPA).

### Notes

This study was approved by the Institutional Animal Care and Use Committee (IACUC) of Kangwon National University, South Korea (Registration no. KW-230629-1), and then conducted in compliance with the UK/EU/US Animal Research Reporting In vivo Experiment (ARRIVE) guidelines. The authors declare no competing financial interest.

### ABBREVIATIONS

FBR	fermented brown rice
RBR	raw brown rice
ND	normal diet
HFD	high-fat diet
LD	low-dose
MD	mid-dose
HD	high-dose
TC	total cholesterol
TG	triglycerides
LDL-C	low-density lipoprotein cholesterol
HDL-C	high-density lipoprotein cholesterol
RTPCR	real-time polymerase chain reaction
PPAR $\gamma$	peroxisome proliferator activated receptor gamma
FABP4	fatty acid binding protein 4
ADIPOQ	adiponectin
GADPH	glyceraldehyde 3-phosphate dehydrogenase
$\Delta\Delta CT$	delta delta cycle threshold
KEGG	Kyoto encyclopedia of genes and genomes
DEGs	differentially expressed genes
FASN	fatty acid Synthase
PPAR $\gamma$	peroxisome proliferator activated receptor gamma
IL6	interleukin 6
PTGS1	prostaglandin-endoperoxide synthase 1

### REFERENCES

- (1) Tham, K. W.; Abdul Ghani, R.; Cua, S. C.; Deerochanawong, C.; Fojas, M.; Hocking, S.; Lee, J.; Nam, T. Q.; Pathan, F.; Saboo, B.; Soegondo, S.; et al. Obesity in South and Southeast Asia—A new consensus on care and management. *Obes Rev.* **2023**, *24* (2), 13520.
- (2) Kang, H. S.; Kim, J. H.; Kim, J. H.; Bang, W. J.; Choi, H. G.; Kim, N. Y.; Park, H. Y.; Kwon, M. J. Unlocking the Protective Potential of Upper Respiratory Infection Treatment Histories against Alzheimer’s Disease: A Korean Adult Population Study. *J. Clin. Med.* **2024**, *13* (1), 260.
- (3) Coutinho, W.; Halpern, B. Pharmacotherapy for obesity: moving towards efficacy improvement. *Diabetol. metab. syndr.* **2024**, *16* (1), 6.
- (4) Rigaudière, J. P.; Jouve, C.; Capel, F.; Patrac, V.; Miguel, B.; Tournadre, A.; Demaison, L. An experimental model of western diet in female Wistar rats leads to cardiac hypoxia related to a stimulated contractility. *Journal of Physiology and Biochemistry* **2024**, *80*, 287.
- (5) Barathikannan, K.; Chelliah, R.; Elahi, F.; Tyagi, A.; Selvakumar, V.; Agastian, P.; Valan Arasu, M.; Oh, D. H. Anti-obesity efficacy of *Pediococcus acidilactici* MNLS in *Canorhabditis elegans* gut model. *Int. J. Mol. Sci.* **2022**, *23* (3), 1276.
- (6) Tyagi, A.; Lim, M. J.; Kim, N. H.; Barathikannan, K.; Vijayalakshmi, S.; Elahi, F.; Ham, H. J.; Oh, D. H. Quantification of Amino Acids, Phenolic Compounds Profiling from Nine Rice

- Varieties and Their Antioxidant Potential. *Antioxidants* **2022**, *11* (5), 839.
- (7) Tyagi, A.; Shabbir, U.; Chelliah, R.; Daliri, E. B. M.; Chen, X.; Oh, D. H. *Limosilactobacillus reuteri* fermented brown rice: A product with enhanced bioactive compounds and antioxidant potential. *Antioxidants* **2021**, *10* (7), 1077.
- (8) Yang, S. T. *Bioprocessing for Value-Added Products from Renewable Resources: New Technologies and Applications*; Elsevier: Amsterdam, The Netherlands, 2011.
- (9) Jemil, I.; Mora, L.; Nasri, R.; Abdelhedi, O.; Aristoy, M.-C.; Hajji, M.; Nasri, M.; Toldrà, F. A peptidomic approach for the identification of antioxidant and ACE-inhibitory peptides in sardinelle protein hydrolysates fermented by *Bacillus subtilis* A26 and *Bacillus amyloliquefaciens* An6. *Food Res. Int.* **2016**, *89*, 347–358.
- (10) Lee, E. M.; Lee, S. S.; Chung, B. Y.; Cho, J. Y.; Lee, I. C.; Ahn, S. R.; Jang, S. J.; Kim, T. H. Pancreatic lipase inhibition by C-glycosidic flavones isolated from *Eremochloa ophiuroides*. *Molecules* **2010**, *15* (11), 8251–8259.
- (11) Kawser Hossain, M.; Abdal Dayem, A.; Han, J.; Yin, Y.; Kim, K.; Kumar Saha, S.; Yang, G. M.; Choi, H. Y.; Cho, S. G. Molecular mechanisms of the anti-obesity and anti-diabetic properties of flavonoids. *Int. J. Mol. Sci.* **2016**, *17* (4), 569.
- (12) Barathikannan, K.; Chelliah, R.; Vinothkanna, A.; Prathiviraj, R.; Tyagi, A.; Vijayalakshmi, S.; Lim, M. J.; Jia, A. Q.; Oh, D. H. Untargeted metabolomics-based network pharmacology reveals fermented brown rice towards anti-obesity efficacy. *npj Sci. Food* **2024**, *8*, 20.
- (13) Barathikannan, K.; Chelliah, R.; Yeon, S. J.; Tyagi, A.; Elahi, F.; Vijayalakshmi, S.; Agastian, P.; Arockiasami, V.; Hawn Oh, D. Untargeted metabolomics of fermented onion (*Allium cepa* L.) using UHPLC Q-TOF MS/MS reveals anti-obesity metabolites and in vivo efficacy in *Caenorhabditis elegans*. *Food Chem.* **2023**, *404*, 134710.
- (14) Lee, M.; Yun, Y. R.; Choi, E. J.; Song, J. H.; Kang, J. Y.; Kim, D.; Lee, K. W.; Chang, J. Y. Anti-obesity effect of vegetable juice fermented with lactic acid bacteria isolated from kimchi in C57BL/6J mice and human mesenchymal stem cells. *Food Funct.* **2023**, *14* (3), 1349–1356.
- (15) Ofofu, F. K.; Elahi, F.; Daliri, E. B. M.; Aloo, S. O.; Chelliah, R.; Han, S. I.; Oh, D. H. Fermented sorghum improves type 2 diabetes remission by modulating gut microbiota and their related metabolites in high fat diet-streptozotocin induced diabetic mice. *J. Funct. Foods* **2023**, *107*, 105666.
- (16) Tamang, J. P.; Cotter, P. D.; Endo, A.; Han, N. S.; Kort, R.; Liu, S. Q.; Mayo, B.; Westerik, N.; Hutkins, R. Fermented foods in a global age: East meets West. *Compr. Rev. Food Sci. Food Saf* **2020**, *19* (1), 184–217.
- (17) Mukherjee, M. Human digestive and metabolic lipases—a brief review. *J. Mol. Catal., B Enzym* **2003**, *22* (5–6), 369–376.
- (18) Georgiev, V. G.; Weber, J.; Kneschke, E.-M.; Denev, P. N.; Bley, T.; Pavlov, A. I. Antioxidant activity and phenolic content of betalain extracts from intact plants and hairy root cultures of the red beetroot *Beta vulgaris* cv. Detroit dark red. *Plant Foods Hum. Nutr.* **2010**, *65*, 105–111.
- (19) De Melo, T.; Lima, P.; Carvalho, K.; Fontenele, T.; Solon, F.; Tomé, A.; De Lemos, T.; da Cruz Fonseca, S.; Santos, F.; Rao, V.; et al. Ferulic acid lowers body weight and visceral fat accumulation via modulation of enzymatic, hormonal, and inflammatory changes in a mouse model of high-fat diet-induced obesity. *Braz. J. Med. Biol. Res.* **2017**, *50*, No. e5630.
- (20) Al-Okbi, S. Y.; Ali, O.; Aly, A. S.; Refaat, D.; Esmail, R. S.; Elbakry, H. F. Management of metabolic syndrome by nutraceuticals prepared from chitosan and ferulic acid with or without beta-sitosterol and their nanoforms. *Sci. Rep.* **2023**, *13* (1), 12176.
- (21) Naowaboot, J.; Piyabhan, P.; Munkong, N.; Parklak, W.; Pannangpetch, P. Ferulic acid improves lipid and glucose homeostasis in high-fat diet-induced obese mice. *Clin. Exp. Pharmacol. Physiol.* **2016**, *43*, 242–250.
- (22) Ye, L.; Hu, P.; Feng, L. P.; Huang, L. L.; Wang, Y.; Yan, X.; Xiong, J.; Xia, H. L. Protective Effects of Ferulic Acid on Metabolic Syndrome: A Comprehensive Review. *Molecules* **2022**, *28*, 281.
- (23) Rodrigues, C. F.; Salgueiro, W.; Bianchini, M.; Veit, J. C.; Puntel, R. L.; Emanuelli, T.; Dernadin, C. C.; Avila, D. S. *Salvia hispanica* L.(chia) seeds oil extracts reduce lipid accumulation and produce stress resistance in *Caenorhabditis elegans*. *Nutr. Metab.* **2018**, *15*, 83.
- (24) Ge, Y.; Shi, Y.; Wei, C.; Uthamapriya, R. A.; Wu, Y.; Cao, L. The effects of quinoa bran dietary fiber on glucose and lipid metabolism and hepatic transcriptome in obese rats. *J. Sci. Food Agric.* **2024**, *104* (5), 2692–2703.
- (25) Cao, S.; Yang, L.; Xie, M.; Yu, M.; Shi, T. Peanut-natto improved obesity of high-fat diet mice by regulating gut microbiota and lipid metabolism. *J. Funct. Foods* **2024**, *112*, 105956.
- (26) Welsh, A.; Hammad, M.; Piña, I. L.; Kulinski, J. Obesity and cardiovascular health. *Eur. J. Prev. Cardiol.* **2024**, *31*, 1029.
- (27) Martinez, O. D. M.; Theodoro, J. M. V.; Grancieri, M.; Toledo, R. C. L.; Queiroz, V. A. V.; de Barros, F. A. R.; Martino, H. S. D. Dry heated whole sorghum flour (BRS 305) with high tannin and resistant starch improves glucose metabolism, modulates adiposity, and reduces liver steatosis and lipogenesis in Wistar rats fed with a high-fat high-fructose diet. *J. Cereal Sci.* **2021**, *99*, 103201.
- (28) Magne, F.; Gotteland, M.; Gauthier, L.; Zazueta, A.; Poeso, S.; Navarrete, P.; Balamurugan, R. The firmicutes/bacteroidetes ratio: a relevant marker of gut dysbiosis in obese patients? *Nutrients* **2020**, *12* (5), 1474.
- (29) Zhao, X.; Fu, Z.; Yao, M.; Cao, Y.; Zhu, T.; Mao, R.; Huang, M.; Pang, Y.; Meng, X.; Li, L.; Zhang, B.; et al. Mulberry (*Morus alba* L.) leaf polysaccharide ameliorates insulin resistance-and adipose deposition-associated gut microbiota and lipid metabolites in high-fat diet-induced obese mice. *Food Sci. Nutr* **2022**, *10* (2), 617–630.
- (30) Somnuk, S.; Komindr, S.; Monkhai, S.; Poolsawat, T.; Nakphaichit, M.; Wanikorn, B. Metabolic and inflammatory profiles, gut microbiota, and lifestyle factors in overweight and normal weight young thai adults. *PLoS One* **2023**, *18* (7), No. e0288286.
- (31) Zhang, M.; Yang, T.; Li, R.; Ren, K.; Li, J.; He, M.; Chen, J.; Yi, S. Q. Gut microbiota of *Suncus murinus*, a naturally obesity-resistant animal, improves the ecological diversity of the gut microbiota in high-fat-diet-induced obese mice. *PLoS One* **2023**, *18* (11), No. e0293213.
- (32) Li, L.; Wang, S.; Zhang, T.; Lv, B.; Jin, Y.; Wang, Y.; Chen, X.; Li, N.; Han, N.; Wu, Y.; Yuan, J. Walnut peptide alleviates obesity, inflammation and dyslipidemia in mice fed a high-fat diet by modulating the intestinal flora and metabolites. *Front. Immunol* **2023**, *14*, 1305656.
- (33) Li, M.; Kang, S. G.; Huang, K.; Tong, T. Dietary Supplementation of Methyl Cedryl Ether Ameliorates Adiposity in High-Fat Diet-Fed Mice. *Nutrients* **2023**, *15* (3), 788.
- (34) Jamar, G.; Estadella, D.; Pisani, L. P. Contribution of anthocyanin-rich foods in obesity control through gut microbiota interactions. *BioFactors* **2017**, *43* (4), 507–516.
- (35) Wang, R.; Wang, L.; Wang, S.; Wang, J.; Su, C.; Zhang, L.; Li, C.; Liu, S. Phenolics from noni (*Morinda citrifolia* L.) fruit alleviate obesity in high fat diet-fed mice via modulating the gut microbiota and mitigating intestinal damage. *Food Chem.* **2023**, *402*, 134232.
- (36) Landgraf, K.; Klötting, N.; Gericke, M.; Maixner, N.; Guinjurado, E.; Scholz, M.; Witte, A. V.; Beyer, F.; Schwartz, J. T.; Lacher, M.; Villringer, A.; et al. The obesity-susceptibility gene TMEM18 promotes adipogenesis through activation of PPAR $\gamma$ . *Cell Rep.* **2020**, *33* (3), 108295.
- (37) Camargo, A.; Meneses, M. E.; Perez-Martinez, P.; Delgado-Lista, J.; Jimenez-Gomez, Y.; Cruz-Teno, C.; Tinahones, F. J.; Paniagua, J. A.; Perez-Jimenez, F.; Roche, H. M.; Malagon, M. M.; et al. Dietary fat differentially influences the lipids storage on the adipose tissue in metabolic syndrome patients. *Eur. J. Nutr.* **2014**, *53*, 617–626.
- (38) Roh, H. C.; Kumari, M.; Taleb, S.; Tenen, D.; Jacobs, C.; Lyubetskaya, A.; Tsai, L. T. Y.; Rosen, E. D. Adipocytes fail to

maintain cellular identity during obesity due to reduced PPAR $\gamma$  activity and elevated TGF $\beta$ -SMAD signaling. *Mol. Metab* **2020**, *42*, 101086.

(39) Baruah, R.; Ray, M.; Halami, P. M. Preventive and therapeutic aspects of fermented foods. *J. Appl. Microbiol.* **2022**, *132* (5), 3476–3489.

(40) Melini, F.; Melini, V.; Luziatelli, F.; Ficca, A. G.; Ruzzi, M. Health-promoting components in fermented foods: an up-to-date systematic review. *Nutrients* **2019**, *11* (5), 1189.

(41) Galimberti, A.; Bruno, A.; Agostinetto, G.; Casiraghi, M.; Guzzetti, L.; Labra, M. Fermented food products in the era of globalization: Tradition meets biotechnology innovations. *Curr. Opin. Biotechnol.* **2021**, *70*, 36–41.